ELSEVIER Science Press

Trans. Nonferrous Met. Soc. China 19(2009) s463−s469

Transactions of Nonferrous Metals Society of China

www.tnmsc.cn

Influence of processing parameters and heat treatment on phase composition and microstructure of plasma sprayed hydroxyapatite coatings

ZHAO Guo-liang(赵国亮)[1], WEN Guang-wu(温广武)[1], WU Kun(吴 昆)[2]

1. School of Materials Science and Engineering, Harbin Institute of Technology (Weihai), Weihai 264209, China;
2. School of Materials Science and Engineering, Harbin Institute of Technology, Harbin 150001, China

Received 10 June 2009; accepted 15 August 2009

Abstract: Air plasma spraying process was employed to fabricate various hydroxyapatite(HA) coatings on titanium substrates. The influence of processing parameters on the phase composition and the microstructure of the obtained coatings was investigated. The effect of heat treatment on as-sprayed coating in terms of the crystallinity and microstructure was also studied. The phase composition of coatings was analyzed by X-ray diffraction(XRD) and FTIR. The surface and cross-section morphologies and microstructure of coatings as well as the morphology of feedstock were evaluated using scanning electron microscope(SEM). The crystallization temperature of amorphous HA phase in as-sprayed coating was examined by using differential thermal analysis(DTA). The results suggest that phase composition and microstructure of as-sprayed HA coatings strongly depend on the spraying parameters, and heat treatment at 760 ℃ for 2 h is one of effective means for increasing the crystallinity and improvement in microstructure of as-sprayed HA coatings.

Key words: hydroxyapatite coatings; plasma spraying; processing parameters; heat treatment

1 Introduction

Hydroxyapatite[$Ca_{10}(PO_4)_6(OH)_2$](HA) has been extensively used as biomedical material due to its good biocompatibility and bioactivity. The similarity of chemical structure between HA and natural bone makes it one of the most attractive materials to treat and replace the broken parts of human bones. However, HA material could not be used in bulk form for load bearing applications due to its poor mechanical properties such as low strength and fracture toughness. So, implants using HA as coatings and metals such as titanium as substrates become the focus because of the combination of superior biological and mechanical properties. HA coatings can not only benefit to the building-up of new tissue but also fix the implants inside the body and protect surrounding bone against metal-ion release from metallic implants[1−3].

The plasma spray process is a very established method to fabricate coatings on titanium and its alloys. The property of plasma sprayed coatings is influenced by a large number of various parameters including feedstock, arc current, arc voltage, main gas flow rate, stand-off distance, substrate and so on[4−5]. On one hand, the decomposition of hydroxyapatite owing to subjection to extremely high temperature causes complicated phase composition in the coatings including crystalline and amorphous HA, calcium phosphates such as tricalcium phosphate(TCP) and tetracalcium phosphate(TTCP) and calcium oxide(CaO)[6−8]. The presence of phases TCP, TTCP and CaO results from the decomposition of HA subjected to high temperature plasma flame. The formation of amorphous calcium phosphate in the coating is owing to the high cool rate of the droplets as well as the relevant intrinsic properties of HA[9]. These impurities (TCP, TTCP and CaO) can lower the bioactivity of HA coatings and the metastable amorphous HA can influence the fixation of implants due to the higher soluble rate in body circumstance. On the other hand, the microstructure of coatings is influenced by plasma spraying parameters too. Therefore, it is critical to control the content of them during the preparation of the plasma sprayed coatings through suitable processing parameters. Furthermore, post treatment for coatings is always carried out after plasma spraying in order to further improve the mechanical property of coatings through releasing the residual stress between the coating and the substrate and the reduction of micro-cracks and pores in coatings[10−12].

Corresponding author: WEN Guang-wu; Tel: +86-631-5687390; E-mail: g.wen@hit.edu.cn; wgw@hitwh.edu.cn

The objective of the present work is to investigate the effect of process parameters and heat treatment on phase composition and microstructure of the plasma sprayed HA coatings.

2 Experimental

2.1 Feedstock and substrate material

The raw HA powder was synthesized by reacting calcium nitrate with diammonia hydro-phosphate[13]. The reaction is as follows:

$$10Ca(NO_3)_2+6(NH_4)_2HPO_4+8NH_4OH \longrightarrow Ca_{10}(PO_4)(OH)_2+20NH_4NO_3+6H_2O \quad (1)$$

The pH value for the reaction was kept around 9 using aqueous ammonia and the temperature was maintained at 35 ℃. The as-synthesized powder was subjected to heat treatment for 2 h at 900 ℃ for further crystallization, which was performed in air in a high-temperature furnace without gas flow. Afterwards, the powder was pressed to compact by a pressure machine and then was crushed into fine particles. At last the powder was sieved into 100−200 mesh for subsequent plasma spraying. Commercial high purity TA2 plates were used as substrates with dimensions of 55 mm×30 mm×2 mm. Prior to spraying, the surfaces of substrates were degreased with acetone to remove contaminants and grit blasted with Al_2O_3 (500 μm) to roughen the surfaces.

2.2 Atmospheric plasma spray

The high purity argon, hydrogen and ordinary argon were used as the main plasma forming gas, auxiliary gas and carrier gas, respectively. The plasma spraying conditions are listed in Table 1.

Table 1 Plasma spraying parameters for HA coatings

Coating	Arc current/ A	Arc voltage/ V	Main gas flow rate/ ($L \cdot min^{-1}$)	Stand-off distance/ mm
C1	500	40	30	80
C2	550	40	30	80
C3	600	40	30	80
C4	600	35	30	90
C5	600	35	40	90
C6	600	40	30	90

2.3 Heat treatment

Heat treatment for the as-sprayed coating was preformed in air in a high-temperature furnace at 760 ℃ for 2 h.

2.4 Characterization

Feedstock and coatings morphologies were examined by JEOL JSM-6390 scanning electron microscope(SEM). The examined cross-section samples were mounted in epoxy resin, followed by grinding using emery papers.

The phase compositions of feedstock and coatings were identified by Siemens D5000 X-ray diffractometer (XRD) with Cu K_α radiation in a 2θ range from 20° to 60°.

A Nicolet-380 spectrometer was used to record the infrared spectra of the coatings. The spectra were measured over 4 000−400 cm^{-1} region with a 1 cm^{-1} resolution.

The crystallization temperature of amorphous HA phase in as-sprayed coating was examined by using L62 DTA of Linseis.

3 Results and discussion

3.1 Characteristics of feedstock

Fig.1(a) shows the morphology of the HA feedstock. It is clear that the shape of the feedstock is irregular and multi-angular, and the size of the feedstock is homogeneous. After heat-treatment at 900 ℃ for 2 h, the as-synthesized powders exhibit high purity and degree of crystallinity. XRD analysis shows that there are not other calcium phosphate or other undesirable phases, such as tricalcium phosphate(TCP) or calcium oxide(CaO) (Fig.1(b)).

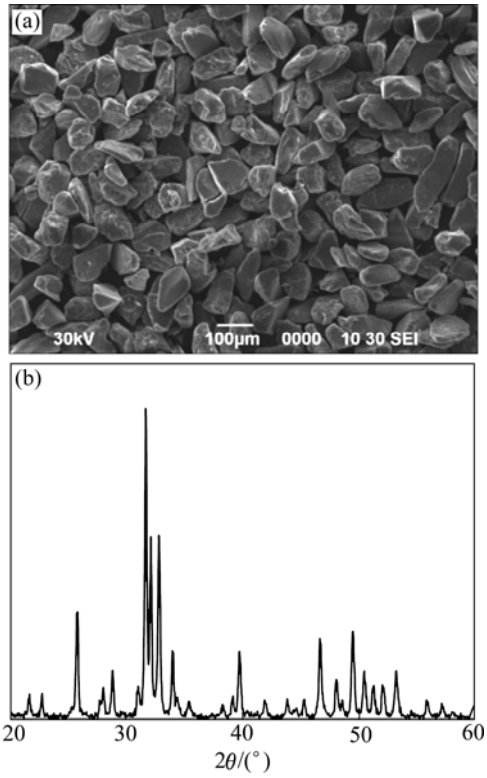

Fig.1 Morphology(a) and phase composition(b) of HA feedstock after heat treatment

3.2 Effects of parameters on phases constitution of coatings

The X-ray diffraction(XRD) patterns of sprayed coating with various currents are shown in Fig.2(a) (coatings C1−C3). It is found that the phases in sprayed coating are almost common, which consist of not only crystalline and amorphous HA but also other contaminations such as α-tri-calcium phosphate (α-TCP), tetra-calcium phosphate(TTCP) and calcium oxide(CaO). However, the intensity of HA peak (211) decreases and that of the peak (002) increases with the increase of current, which may indicate the content of HA reduces[14]. The phases of coatings C4 and C6 prepared at arc voltage of 35 V and 40 V are shown in Fig.2(b). The patterns indicate the two coatings are composed of HA, α-TCP, TTCP and CaO. The intensity of HA peak (211) of coating C4 pattern is remarkably higher than that of the counterpart of coating C6 pattern, which indicates the amount of HA in the coating C4 is more than that in the coating C6. Correspondingly, the content of CaO of coating C4 is less than that of coating C6. The only difference between the coatings C5 and C4 is the main gas flow rate. It is probably just this difference of the main gas flow rate between the two coatings that gives rise to the distinction of phase content. In addition, through comparison it is easy to find that the content of crystal HA in coating C3 is more than that in coating C6.

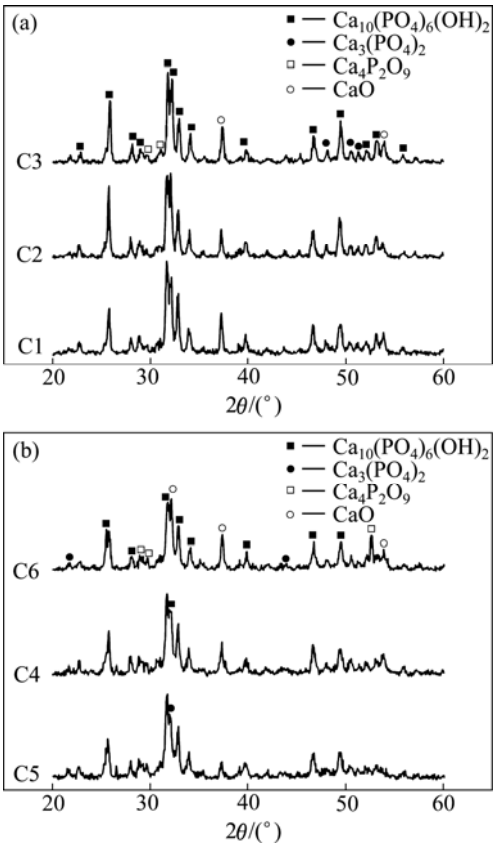

Fig.2 Phase composition of coatings with different plasma spraying parameters

It is clear that after plasma spraying HA is decomposed to different degree. In addition, the increase of the current, voltage and main gas flow rate intensifies the decomposition degree of HA although the resultants are not common at all. The enhancement of decomposition in HA predominantly results from the increase of the amount of melting HA powders or the melting degree of the HA powders due to the increased temperature of plasma flame. The effect of stand-off on the plasma sprayed HA coating is not very prominent. The reason may be the difference between the two stand-off distances is not enough to influence the phase transformation intensely. But, it is worth noting that when the stand-off distance is enlarged from 80 to 90 mm, the content of crystalline HA increases rather than decreases owing to the increase of amorphous HA or other reasons. According to traditional viewpoint, as the stand-off distance increases, the enhancement of the amount of amorphous HA and TCP leads to the decrease of crystalline HA because increasing the stand-off distance can extend the dwelling time in plasma flame, which results in the increase of the extent of melting HA particles. The nature of the phenomenon is still not very clear but maybe relates to phase transformation during cooling process.

3.3 Morphology and microstructure of coatings

The surface and cross-section morphologies of all the HA coatings (C1−C6) are shown in Fig.3 and Fig.4, respectively. It is clear from the surface morphologies that all coatings are porous and contain fine spherical particles. The size of the particles is only around or less than 10 μm, which is smaller than that of all the feedstock remarkably. The surface morphologies also show that most of the particles have been melted and formed splats of coatings during impact on the substrates surface. In addition, cracks are absent in the surface of the coatings.

Certainly, the differences in the porosity, degree of melting and number of fine particles are present in coatings. The scanning electron micrographs of HA coatings sprayed with different arc currents (500, 550 and 600 A) are shown in Fig.3. It can be found obviously that the particles in Fig.3(b) are less than those in Fig.3(a) but larger than those in Fig.3(c) although the difference in the porosity of the three coatings is hardly distinguished. The difference in the degree of melting is observed more obviously in the morphologies of cross-sections as shown in Fig.4. From it, one can recognize that the arc current can strongly influence the surface morphology and microstructure of the coatings.

The surface and cross-section morphologies of the coatings sprayed at different main gas flow rates (30 and 40 L/min) are exhibited in Figs.3(d), (e) and Figs.4(d)

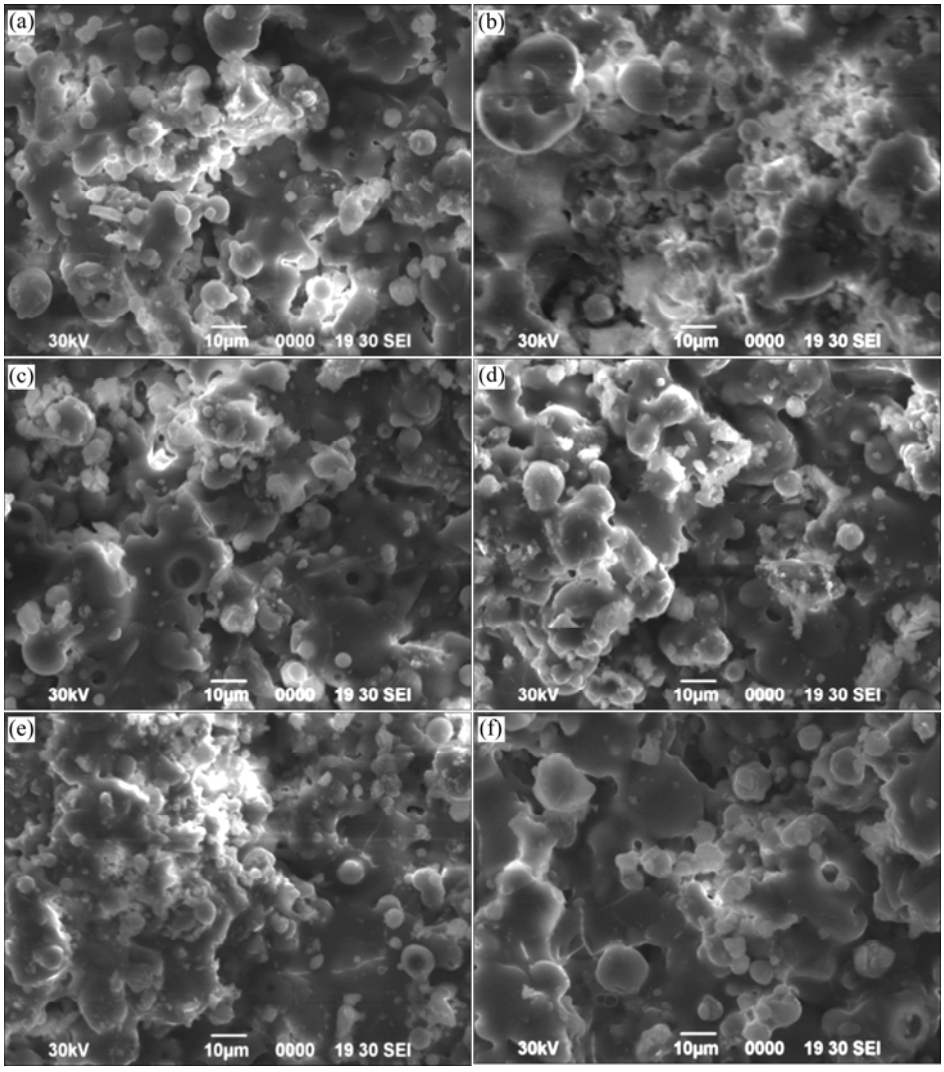

Fig.3 SEM micrographs showing surface morphologies of coatings: (a) C1; (b) C2; (c) C3; (d) C4; (e) C5; (f) C6

and (e), respectively. By contrast, not only the number of porous in the coating sprayed at 40 L/min is less than that in the coating sprayed at 30 L/min, but also the size of porous in the coating sprayed at 40 L/min is smaller remarkably than that in the coating sprayed at 30 L/min. And the degree of melting of the coating sprayed at 40 L/min is slightly higher than that of the coating sprayed at 30 L/min, which can be seen in the cross-section morphologies.

As for the influence of arc voltage on the microstructure of the HA coatings, it can be recognized by comparison of Figs.3(d), (f) and Figs.4(d) and (f). The melting degree of the particle in the coating sprayed at arc voltage of 40 V is better than that in the coating sprayed at arc voltage of 35 V, which is demonstrated more sufficiently in the morphologies of cross-section.

The spraying parameters used in the present work strongly influence not only the resultant phases but also the microstructure of the as-sprayed coatings. The increase in arc current, arc voltage and main gas flow rate can enhance the temperature of plasma flame and accordingly lead to more sufficient melting of the injected HA particles. The bonding among splats and between coating and substrate becomes better, and larger cracks are absent in coatings and interfaces. Increasing stand-off distance can prolong the dwelling time of particles in the high temperature plasma jet and the melting degree of the particles can be accordingly increased.

The presence of fine spherical particles in the surface and inside of the coatings was detected by the SEM. However, this case is far different from that mentioned in literatures. The particles in present work are not the particles which are too large to be melted in plasma flame due to short duration during the spraying process. Contrarily, the size of most of particles is around or less than 10 μm and far smaller than that of the feed-stock. Accordingly, the formation of these particles could be explained that during or after melting, part of the melting droplets are separated into many fine droplets due to the action of the high speed plasma jet and these fine droplets are cooled and solidified before compact on

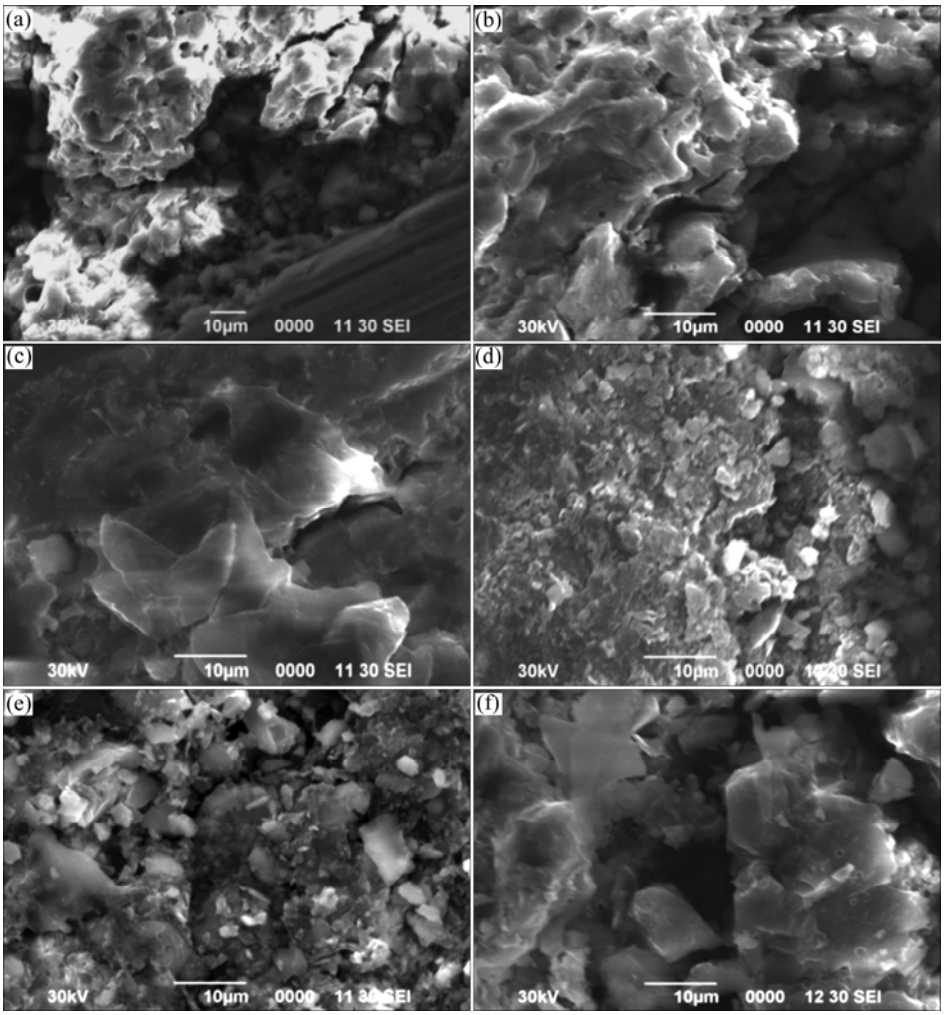

Fig.4 SEM micrographs showing cross-section microstructures of coatings: (a) C1; (b) C2; (c) C3; (d) C4; (e) C5; (f) C6

the substrate owing to lower thermal capacity and the larger droplets formed splats. Therefore, there are fine spherical particle preserving in the surface or in the coatings.

3.4 Result of heat treatment

The broadened peaks shown in the XRD patterns (Fig.2) indicate that there exist a large amount of amorphous HA phases in the coating C1, and the crystallinity of which is the lowest among the examined coatings. In the present work, heat-treatment is employed to improve the crystallinity of the coating C1. The changes in the surface and cross-section morphology and microstructure of the coating are investigated.

Fig.5 shows the XRD pattern of the coatings treated at 760 ℃ for 2 h. From the pattern, one can observe all the peaks are very sharp and the intensity of HA peaks is obviously stronger than that of untreated coating, which indicates that most of amorphous HA has transformed into crystalline HA. However, the CaO and TTCP phases still exist in the as-treated coating. Fig.6 demonstrates

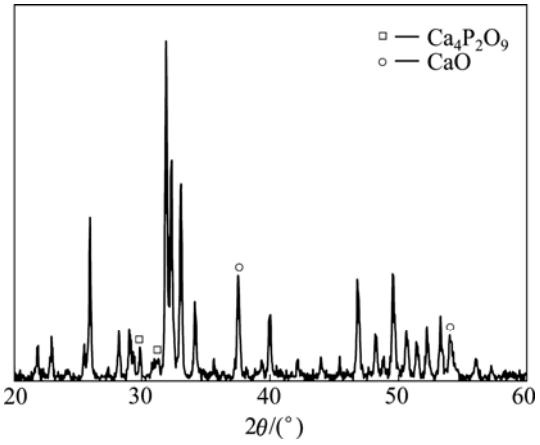

Fig.5 XRD pattern of HA coating treated at 750 ℃ for 2 h

the FTIR spectra of the treated and untreated coatings. The strong band at 631 cm^{-1} can be unambiguously assigned to the lattice O—H stretching vibration. Weaker bands were also observed at 3 571 cm^{-1}, which also suggested the existence of hydroxyl group. After heat treatment, the content of OH^- group increases obviously.

These results are consistent with many other reports[15−17]. However, the peak intensity of the as-treated coating increases in comparison with the untreated coating. This result is consistent with that of XRD and further proves the occurrence of phase transformation from amorphous HA to crystalline HA during the heat treatment.

In addition, the microstructure of the coating and interface bonding is strongly influenced by the heat treatment too. Through the comparison between the microstructure of the untreated and treated coatings, it is not difficult to see that after heat treatment the pores decrease and melting degree increases remarkably and the adhesion of the coating is subsequently improved. And the coating/substrate interface bonding is also improved to some extent. The surface, cross-section and interface morphologies and microstructure are shown in Fig.7.

Heat treatment has been employed to crystallize as-sprayed coatings in many cases. But the treatment temperatures were dramatically distinguished, and the range was always changed from 600 ℃ to 900 ℃[10,18]. In addition, the treatment at different temperatures was always effective to different degrees. Therefore, it can be concluded that the temperature of transformation from amorphous HA to crystalline HA is not a specific temperature point or limited temperature zone but a broader temperature zone. This may be verified by the

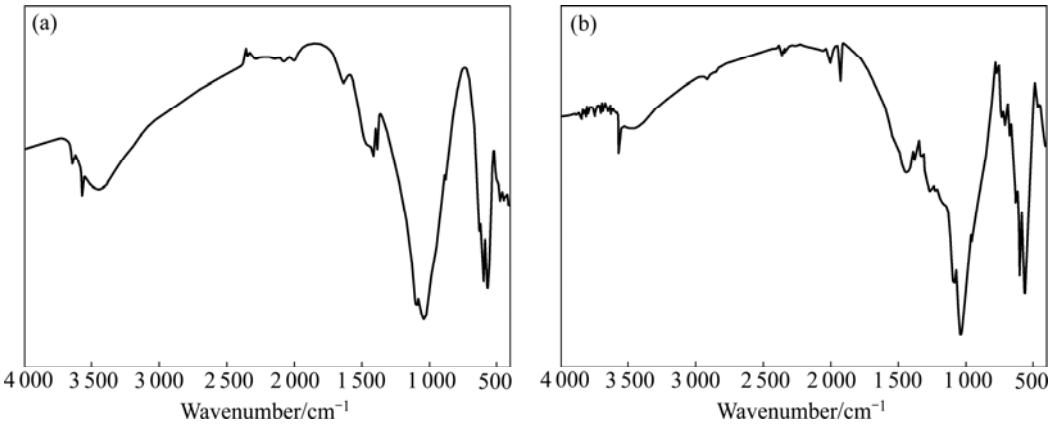

Fig.6 FTIR spectra of as-treated (a) and as-sprayed (b) coatings

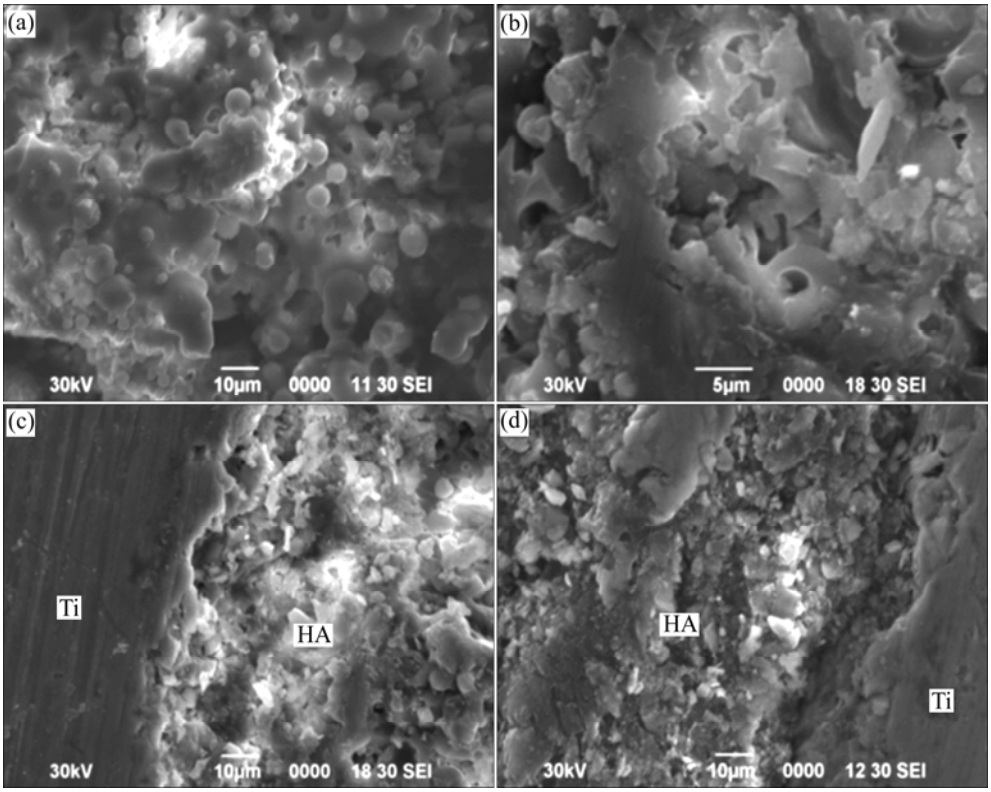

Fig.7 SEM micrographs of as-treated and as-sprayed coatings: (a), (b) and (c) Morphologies of surface, cross-section and interface of as-treated coating; (d) Interface morphologies of as-sprayed coating

DTA curve (as shown in Fig.8), in which there are no obvious exothermic peaks during heating process. The main reason to select 760 ℃ as heat treatment temperature is to prevent as-transformed crystalline HA from changing into other impurity phases at higher temperature[12]. FENG et al[5] investigated the phase transformation in plasma sprayed HA coatings by DSC. They believed that under a certain heating condition amorphous HA could involve three intermediate reactive steps and form HA, HA+TTCP and HA+CaO, respectively. The final products of heat treated coating in present work are exactly consistent with the results of that investigation. The heat treatment of the as-spayed coating resulted in not only the phase transformation but also the improvement of microstructure of coatings which could correspond to increase in adhesion and cohesion of the coating system.

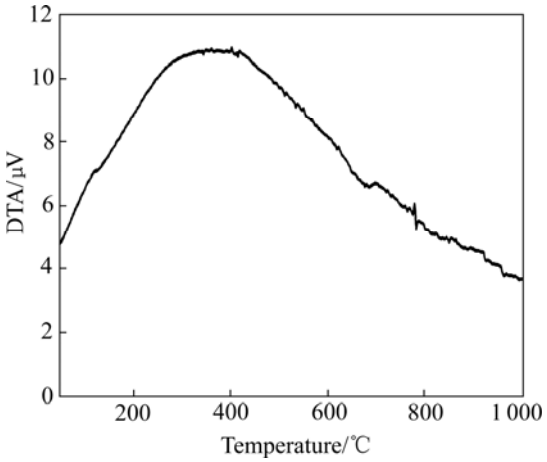

Fig.8 DTA curve of HA coating C1

4 Conclusions

1) The decomposition of HA can not be avoided during plasma spraying process. The resultant phases in the as-sprayed coating mainly consist of HA, TCP, TTCP and CaO.

2) The increase in arc current, arc voltage, main gas flow rate and stand-off distance can deteriorate the HA phase decomposition.

3) The surface and cross-section morphologies and microstructure of the coatings are improved with the increase in arc current, arc voltage, main gas flow rate and stand-off distance and decrease in the size of feedstock.

4) Sufficient melting of the feedstock may not avoid the presence of a certain number of spherical particles in as-sprayed coatings owing to the separation of melting particles subjected to the plasma jet.

5) 760 ℃ is an appropriate heat treatment temperature for increasing the crystallinity of HA coatings and improvement of the microstructure of HA coatings.

References

[1] GROSS K A, BERNDT C C. Thermal processing of hydroxyapatite for coating production [J]. Biomedical Material Research, 1998, 39: 580−587.

[2] KHOR K A, WANG Y, CHEANG P. Thermal spraying of functionally graded coatings for biomedical applications [J]. Surface Engineering, 1998, 142: 159−164.

[3] FANG J C, XU W J, ZhAO Z Y, ZENG H P. In-flight behaviors of ZrO_2 particle in plasma spraying [J]. Surface and Coatings Technology, 2007, 201(9−11): 5671−5675.

[4] ZHAO L D, SEEMANN K, FISCHER A, LUGSCHEIDER E. Study on atmospheric plasma spraying of Al_2O_3 using on-line particle monitoring [J]. Surface and Coatings Technology, 2003, 168(2−3): 186−190.

[5] FENG C F, KHOR K A, LIU E J, CHEANG P. Phase transformations in plasma sprayed hydroxyapatite coatings [J]. Scripta Materialia, 2000, 42: 103−109.

[6] INAGAKI M, KAMEYAMA T. Phase transformation of plasma-sprayed hydroxyapatite coating with preferred crystalline orientation [J]. Biomaterials, 2007, 28(19): 2923−2931.

[7] RENGHINI C, GIRARDIN E, FOMIN A S, MANESCA A, SABBIONI A, BARINOV S M, KOMLVLEV V S, ALBERTINI G, FIORI F. Plasma sprayed hydroxyapatite coatings from nano-srtructured granules [J]. Mater Sci Eng B, 2008, 152(1/3): 86−90.

[8] WENG Jie, LIU Xiao-guang, LI Xu-dong, ZHANG Xing-dong. Intrinsic factors of apatite influencing its amorphization during plasma-spray coating [J]. Biomaterials, 1995, 16: 39−44.

[9] YANG Y C. Influnce of residual stress on bonding strength of the plasma-sprayed hydroxyapatite coating after the vacuum heat treatment [J]. Surface and Coatings Technology, 2007, 201: 7187−7193.

[10] CAO Yang, WENG Jie, CHEN Ji-yong. Water vapour-treated hydroxyapatite coatings after plasma spraying and their characteristics [J]. Biomaterials, 1996, 17: 419−424.

[11] CHEN Chuan-zhong, WANG Dian-gang, HE Bao-quan. Influence of laser remelting on the microstructure and phases constitution of plasma sprayed hydroxyapatite coatings [J]. Applied Surface Science, 2005, 250: 98−103.

[12] KWEH S W K, KHOR K A, CHEANG P. The production and characterization of hydroxyapatite (HA) powders [J]. Journal of Materials Processing Technology, 1999, 89/90: 373−377.

[13] MORKS M F, KOBAYASHI A. Effect of gun current on the microstructure and crystallinity of plasma sprayed hydroxyapatite coatings [J]. Applied Surface Science, 2007, 253: 7136−7142.

[14] SUN L M, CHRISTOPHER C B, CLARE P. Grey, phase, structural and microstructural investigation of plasma sprayed hydroxyapatite coatings [J]. Mater Sci Eng A, 2003, 360(1−2): 70−84.

[15] PARK E, ROBERT A, CONDRATE S, LEE D H. Infrared spectral investigation of plasma spray coated hydroxyapatite [J]. Materials Letters, 1998, 36: 38−43.

[16] WU Zhen-jun, HE Li-ping, CHEN Zong-zheng. Fabrication and characterization of hydroxyapatite/Al_2O_3 biocompostite coating on titanium [J]. Trans Nonferrous Met Soc China, 2006, 16(2): 259−266.

(Edited by YUAN Sai-qian)